Program Digest, 2019 IEEE International Ultrasonics Symposium (IUS)
Glasgow, Scotland, October 6-9, 2019

Finite Element Analysis of SAW Propagation Characteristics in c-plane (0001) and a-plane (11-20) AlScN Thin Films

1st Niclas M. Feil
Department of Sustainable Systems Engineering - INATECH
University of Freiburg
Freiburg, Germany
niclas.feil@inatech.uni-freiburg.de

2nd Nicolas Kurz
Department of Sustainable Systems Engineering - INATECH
University of Freiburg
Freiburg, Germany
nicolas.kurz@inatech.uni-freiburg.de

3rd Daniel F. Urban
Fraunhofer Institute for Mechanics of Materials IWM
Freiburg, Germany
daniel.urban@iwm.fraunhofer.de

4th Abdullah Altayara
Department of Sustainable Systems Engineering - INATECH
University of Freiburg
Freiburg, Germany
altayaa@tf.uni-freiburg.de

5th Bjoern Christian
Department of Sustainable Systems Engineering - INATECH
University of Freiburg
Freiburg, Germany
bjoern.christian@inatech.uni-freiburg.de

6th Anli Ding
Fraunhofer Institute for Applied Solid State Physics IAF
Freiburg, Germany
anli.ding@iaf.fraunhofer.de

7th Agnė Žukauskaitė
Fraunhofer Institute for Applied Solid State Physics IAF
Freiburg, Germany
agne.zukauskaite@iaf.fraunhofer.de

8th Oliver Ambacher
Department of Sustainable Systems Enigineering - INATECH
University of Freiburg
Fraunhofer Institute for Applid Solid States Physics IAF
Freiburg, Germany
oliver.ambacher@inatech.uni-freiburg.de

***Abstract*—$Al_{1-x}Sc_xN$ (AlScN) is known for its large elastic and piezoelectric constants and thus is a favorable material for applications in novel radio frequency (RF) components. We investigated a-plane AlScN on r-plane Al_2O_3 (AlScN(11-20)/Al_2O_3(1-102)). The surface acoustic wave (SAW) propagation properties of AlScN(11-20)/Al_2O_3(1-102) and AlScN(11-20)/Al_2O_3(1-102) were analyzed using finite element method (FEM) simulations and the results were compared. Rayleigh-type and Sezawa-type wave modes were identified and the acoustic parameters such as phase velocity, electromechanical coupling coefficient, and reflectivity were evaluated. An increased effective coupling of 5.5 % was detected for Rayleigh-type waves on AlScN(11-20)/Al_2O_3(1-102). The Sezawa-type modes show an even higher coupling up to 6.2 %. Furthermore, we detected increased reflectivity of AlScN(11-20) films compared to c-plane AlScN(0001). Our results reveal the potential of using a-plane AlScN for increasing the electromechanical coupling, which is needed for the upcoming piezo-acoustic filter requirements.**

***Index Terms*—Thin Film, SAW Resonator, FEM, a-plane, AlScN**

I. Introduction

Wurtzite-type aluminium nitride (w-AlN) has become a well-established material for RF filters and oscillators, in particular for mobile communication elements such as duplexers [1], [2]. In 2009, Akiyama et al. [3] observed a strong enhancement of the piezoelectric response of w-AlN by cation substitution with scandium (Sc). The resulting ternary nitride AlScN can be sputter-deposited as a thin film on various substrates. A special substrate of interest for high-frequency surface acoustic wave (SAW) resonators is sapphire (Al_2O_3). It can be produced cost-effectively in good quality and provides high phase velocities due to its large stiffness coefficients. In fact, highly crystalline piezoelectric AlScN can be deposited via magnetron sputter epitaxy [4] on Al_2O_3. Until now, the main focus for SAW applications has been on c-axis-oriented AlScN(0001) films. The electromechanical coupling of wurtzite-type piezoelectric thin films can be further improved by aligning the c-axis with the SAW propagation direction. This has previously been shown for AlN and GaN by growing the a-plane crystal orientation on r-plane Al_2O_3 substrate [5], [6] and the transfer to AlScN has recently been discussed theoretically by neglecting the electrodes [7]. For obtaining more detailed information, we investigated the acoustic properties of AlScN(11-20)/Al_2O_3(1-102) SAW resonators using the finite element method (FEM) including the interditigal transducer (IDT). We used latest experimentally extracted material parameters of $Al_{1-x}Sc_xN$ [8] for $x = 0.32$ and density functional theory (DFT) predictions (unpublished) [9] for even higher Sc content, i.e. $x = 0.41$.

TABLE I
THE ELASTIC (C_{ij}), DIELECTRIC (ϵ_{ij}) AND PIEZOELECTRIC (e_{ij}) PARAMETERS FOR Al_2O_3 [10], AlN [11], $Al_{0.68}Sc_{0.32}N$ [8], AND $Al_{0.59}Sc_{0.41}N$ [9] USED IN THE FEM SIMULATIONS IN THIS WORK.

	Al_2O_3	AlN	$Al_{0.68}Sc_{0.32}N$	$Al_{0.59}Sc_{0.41}N$
C_{11} / GPa	494	396	307	291
C_{33} / Gpa	496	373	230	176
C_{12} / GPa	158	137	147	162
C_{13} / Gpa	114	108	123	132
C_{14} / Gpa	-23	-	-	-
C_{44} / Gpa	145	116	110	105
e_{33} / Cm^{-2}	-	1.55	2.8	3.21
e_{15} / Cm^{-2}	-	-0.48	-0.23	-0.28
e_{31} / Cm^{-2}	-	-0.58	-0.69	-0.78
ϵ_{11}/ϵ_0	9.34	10.3	16.9	27.9
ϵ_{33}/ϵ_0	11.54	10.3	16.8	27.9
ρ / Kgm^{-3}	3986	3212	3320	3409

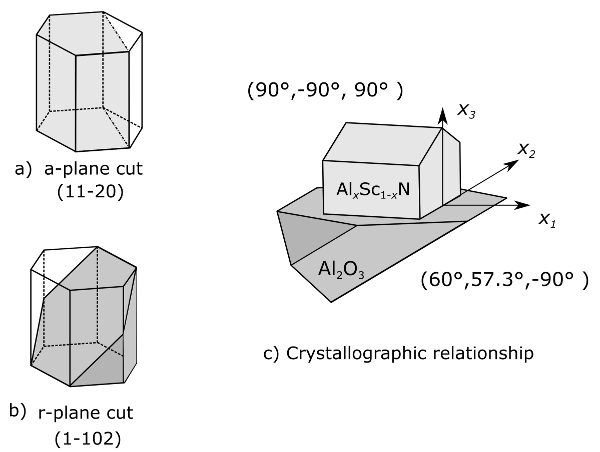

Fig. 1. Crystallographic orientations of thin film and substrate. a) The a-plane cut (11-20) for AlScN thin film, b) the r-plane cut (1-102) for Al_2O_3 as substrate and c) epitaxial relationship between thin film and substrate with respective Euler angles (Bunge-convention).

II. EPITAXIAL RELATIONSHIP

In order to compute the acoustic properties of crystals, the orientations of the respective materials in the model need to be taken into account, i.e. the crystallographic axes of the thin film and the substrate have to be transformed into new coordinate systems. In this work, the orientations are represented as Euler angles [12], defined by three angles with corresponding rotations around the new axis. In a global coordinate system for the FEM study, the wave propagation direction is defined as x_1 and the surface normal as x_3. The orientations for the AlScN(0001)/Al_2O_3(0001) system are transformed according to the coincidence site lattice stacking of the two crystals, resulting in the Euler angles (0°, 0°, 0°) for AlScN(0001) and (30°, 0°, 0°) for Al_2O_3(0001) [13]. In the case of AlScN(11-20)/Al_2O_3(1-102), an ideal relationship of the a-plane for AlScN with the r-plane of Al_2O_3 is assumed [13], illustrated in Figure 1. This leads to the Euler angles (90°, -90°, 90°) for AlScN(11-20) and (-60°, 57.3°, 90°) for Al_2O_3(1-102), respectively.

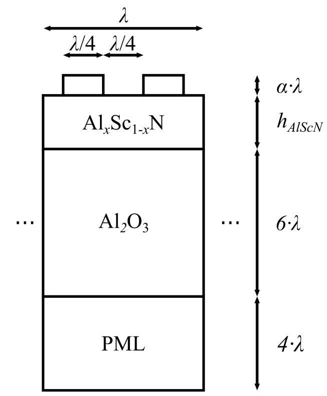

Fig. 2. Geometry of the 2D simulation model. The penetration depth of the surface waves is only a few wavelengths, therefore the substrate is close to several wavelengths thick. The film thickness is defined as $h_{\mathrm{AlScN}} = 1\,\mu$m.

III. SIMULATION MODEL

The acoustic properties were computed using a 2D FEM model. The material parameters used for the simulations are summarized in Table I. Periodicity of the interdigital transducer in SAW resonators allows the use of periodic boundary condition from the left and right of the modeled structure. The AlScN film thickness was set to $h_{\mathrm{AlScN}} = 1\,\mu$m and the remaining geometrical parameters were defined as a function of the wavelength λ. The geometry of the FEM model and the defined geometric parameters are shown in Figure 2. Isotropic material parameters for Cu [14] were used for the electrodes and the normalized thickness was set as $\alpha_{\mathrm{Cu}} = 0.04$. A perfectly matched layer (PML) at the lower edge was defined to avoid reflection of waves at the lower part of the model. The normal modes of the defined geometry were computed for wavelengths between $1 - 10$ μm via an eigenfrequency analysis. Symmetric and anti-symmetric waves with respect to displacement in x_3 direction were calculated for the 1st (Rayleigh-type) and the 2nd (Sezawa-type) wave mode. The phase velocity v_{phase} and reflectivity r were then extracted from the symmetric eigenfrequency f_{sym} and anti-symmetric eigenfrequency f_{asym} [15]:

$$v_{\mathrm{phase}} = \frac{f_{\mathrm{sym}} + f_{\mathrm{asym}}}{2} \cdot \lambda \tag{1}$$

$$r = \pi \frac{f_{\mathrm{asym}} + f_{\mathrm{sym}}}{f_{\mathrm{asym}} - f_{\mathrm{sym}}}. \tag{2}$$

The electrical admittance was obtained in the frequency domain analysis and the effective electromechanical coupling k^2_{eff} was calculated from the serial resonance f_r and the parallel resonance f_a:

$$k^2_{\mathrm{eff}} = \frac{f_a^2 - f_r^2}{f_a^2}. \tag{3}$$

IV. Results and Discussion

In the following, $Al_{1-x}Sc_xN(0001)/Al_2O_3(0001)$ is referred to as c-plane $Al_{1-x}Sc_xN$ and $Al_{1-x}Sc_xN(11\text{-}20)/Al_2O_3(1\text{-}102)$ as a-plane $Al_{1-x}Sc_xN$. At first we studied the influence of the Sc concentration on v_{phase} and k^2_{eff} obtained by the equations (1) and (3) of the Rayleigh-type wave mode in a-plane $Al_{1-x}Sc_xN$ with $x = 0$, 0.32, and 0.41, shown in Figure 3. The phase velocity in Figure 3a decreases for all concentrations up to $h/\lambda = 0.6$ and then remains approximately constant. The reason for this lies in the penetration depth of the surface waves, which is limited to roughly one wavelength. Therefore, for smaller wavelengths, the total displacement components are concentrated in the thin film and the influence of the substrate decreases. The phase velocity decreases faster with increasing Sc content due to the decreasing stiffness coefficients when Sc concentration increases in AlScN (see Table I). The incorporation of Sc into AlN clearly results in an increase of k^2_{eff} for each computed normalized thickness h_{AlScN}/λ, shown in Figure 3b. Furthermore, there is a region between normalized thickness $h_{\text{AlScN}}/\lambda = 0.1$ to 0.3, in which k^2_{eff} shows a sharp global maximum. This maximum increases with larger Sc concentrations and reaches $k^2_{\text{eff}} \approx 5.8\,\%$ for $x = 0.41$. The increase in k^2_{eff} may be influenced, in particular, by the higher piezoelectric component e_{33} at higher Sc concentrations (see Table I).

The comparison between c-plane $Al_{0.59}Sc_{0.41}N$ and a-plane $Al_{0.59}Sc_{0.41}N$ films with respect to v_{phase} and k^2_{eff} is shown in in Figure 4a and 4b, respectively. The Rayleigh-type and the Sezawa-type wave mode is indicated by the circles and triangles, respectively. The phase velocity for both orientations is quite similar and shows nearly the same dispersion for c-plane and a-plane AlScN. In Figure 4a, the coupling of the 1st mode reaches its maximum of approximately $k^2_{\text{eff}} \approx 1.8\,\%$ at $h_{\text{AlScN}}/\lambda = 0.4$, while the 2nd order waves have an increased coupling of about $k^2_{\text{eff}} \approx 4\,\%$ at $h_{\text{AlScN}}/\lambda = 0.85$. In comparison, the properties of a-plane $Al_{0.59}Sc_{0.41}N$ in Figure 4b show improved acoustic characteristics: The electromechanical coupling for waves of 1st mode increases to $k^2_{\text{eff}} = 5.8\,\%$ at $h_{\text{AlScN}}/\lambda = 0.2$. Please note that both the values of k^2_{eff} and v_{phase} are large, which is of advantage for next generation RF-filters. On the other side, waves of the 2nd mode exhibit increased coupling in a long wavelength range, the phase velocities here reach approximately $v_{\text{phase}} \approx 6\,\text{kms}^{-1}$ with $k^2_{\text{eff}} \approx 6.2\,\%$ at $h/\lambda = 0.4$.

The reflectivity r was determined using the equation (2) and is given for a-plane and c-plane $Al_{0.59}Sc_{0.41}N$ as a function of normalized thickness h_{AlScN}/λ in Figure 5. Comparing the 1st mode of c-plane and a-plane $Al_{0.59}Sc_{0.41}N$, an increase of r in a-plane $Al_{0.59}Sc_{0.41}N$ for all examined normalized thicknesses h_{AlScN}/λ is found. A maximum of $r = 20\,\%$ in the range of $h_{\text{AlScN}}/\lambda = 0.1$ to 0.3 is observed, which is exactly the range of high coupling coefficients (see figure 3). For a-plane AlScN, the reflectivity of the 2nd mode is also increased compared to c-plane AlScN in the range $h_{\text{AlScN}}/\lambda = 0.3$ to 0.6.

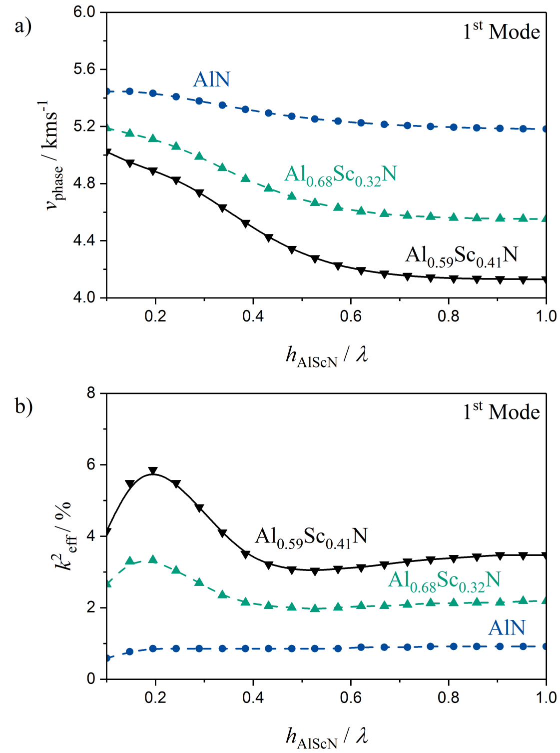

Fig. 3. FEM results for $Al_{1-x}Sc_xN(11\text{-}20)/Al_2O_3(1\text{-}102)$ with $x = 0$ (blue circles), 0.32 (green triangles), and 0.41 (black inverted triangles) Rayleigh-type (1st) wave mode in SAW resonators with Cu electrodes (normalized thickness $\alpha_{\text{Cu}} = 0.04$). a) Phase velocity and b) electromechanical coupling as a function of normalized film thickness.

The increased reflectivity is particularly relevant for the acoustic mirrors. Due to the higher reflectivity, more acoustic energy per transducer finger can be back-reflected, thus giving options to lower the total number of mirror fingers for a-plane AlScN compared to c-plane AlScN, which could reduce the required device area.

V. Summary and Conclusion

In this study, the acoustic properties of $AlScN(0001)/Al_2O_3(0001)$ and $AlScN(11\text{-}20)/Al_2O_3(1\text{-}102)$ based SAW resonators as a function of the normalized film thickness h_{AlScN}/λ were determined via FEM simulation. Our results show an increase of the effective electromechanical coupling k^2_{eff} and the reflectivity r for $Al_{0.59}Sc_{0.41}N(11\text{-}20)/Al_2O_3(1\text{-}102)$, while the trend of the phase velocity v_{phase} of the two thin film orientations is similar. We detected a maximum in effective electromechanical coupling for Rayleigh-type waves in $Al_{0.59}Sc_{0.41}N(11\text{-}20)/Al_2O_3(1\text{-}102)$ of $k^2_{\text{eff}} \approx 5.8\,\%$ at $h_{\text{AlScN}}/\lambda \approx 0.2$. We have also found the existence of Sezawa-type waves in $Al_{0.59}Sc_{0.41}N(11\text{-}20)/Al_2O_3(1\text{-}102)$ with a high coupling of approximately $k^2_{\text{eff}} \approx 6.2\,\%$ and large phase velocity $v_{\text{phase}} \approx 6\,\text{kms}^{-1}$ at $h_{\text{AlScN}}/\lambda = 0.4$. The comparison between the acoustic properties of $Al_{0.59}Sc_{0.41}N(0001)/Al_2O_3(0001)$ and $Al_{0.59}Sc_{0.41}N(11\text{-}20)/Al_2O_3(1\text{-}102)$ based SAW resonators

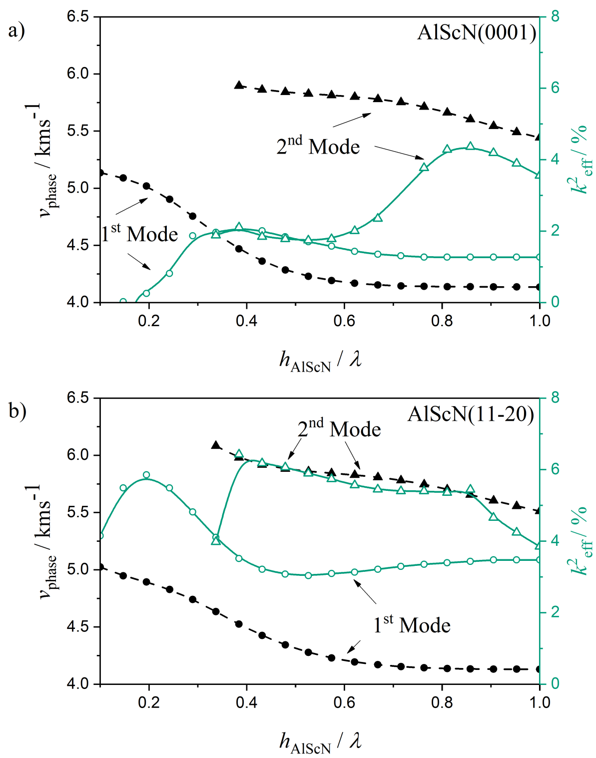

Fig. 4. FEM results for two different AlScN orientations with normalized electrode thickness $\alpha_{Cu} = 0.04$. Comparison of phase velocity (filled symbols) and effective electromechanical coupling coefficient (unfilled symbols) with 1st mode (circles) and 2nd mode (triangles) for a) $Al_{0.59}Sc_{0.41}N(0001)/Al_2O_3(0001)$ and b) $Al_{0.59}Sc_{0.41}N(11\text{-}20)/Al_2O_3(1\text{-}102)$ SAW resonators.

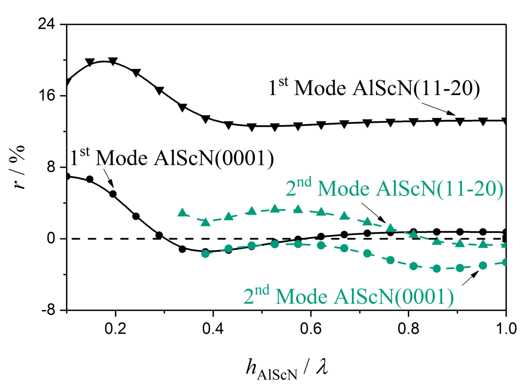

Fig. 5. Computed reflectivity for $Al_{0.59}Sc_{0.41}N(0001)/Al_2O_3(0001)$ and $Al_{0.59}Sc_{0.41}N(11\text{-}20)/Al_2O_3(1\text{-}102)$ based SAW resonators with normalized electrode thickness $\alpha_{Cu} = 0.04$.

underlines the outstanding character and reveals a tripling of the maximum in coupling for the Rayleigh-type waves, while the increase of the maximum in k^2_{eff} for the Sezawa-type waves is almost 50 % higher for $Al_{0.59}Sc_{0.41}N(11\text{-}20)/Al_2O_3(1\text{-}102)$. The reflectivity r of Rayleigh-type waves for $Al_{0.59}Sc_{0.41}N(11\text{-}20)/Al_2O_3(1\text{-}102)$ resonators showed a maximum of approximately $r \approx 20\,\%$ at $h_{\text{AlScN}}/\lambda = 0.2$ and is thus almost three times as high compared to the maximum reflectivity r for $Al_{0.59}Sc_{0.41}N(0001)/Al_2O_3(0001)$ of $r \approx 8\,\%$. Our results reveal the potential of AlScN(11-20) thin films for high frequency SAW resonators with increased bandwidth to be realized in the future.

Acknowledgement

This work was partially supported by the COMET K1 center ASSIC (Austrian Smart Systems Integration Research Center). The COMET (Competence Centers for Excellent Technologies) program is supported by BMVIT, BMWFW, and the federal provinces of Carinthia and Styria. The authors would like to thank Dr. Thomas Metzger (Qualcomm Germany RFFE GmbH) for fruitful scientific discussions.

References

[1] G. Piazza, V. Felmetsger, P. Muralt, R. H. Olsson III, and R. Ruby, “Piezoelectric aluminum nitride thin films for microelectromechanical systems” MRS Bulletin, vol. 37, no. 11, pp. 10511061, 2012
[2] R. M. Aghdam, Growth and properties of AlScN thin films for microwave transducers and piezoelectric energy harvesting, Ph.D. dissertation, Ceramics Laboratory, École Polytechnique Fédérale de Lausanne, Lausanne, 2014
[3] M. Akiyama, T. Kamohara, K. Kano, A. Teshigahara, Y. Takeuchi, and N. Kawahara, “Enhancement of piezoelectric response in scandium aluminum nitride alloy thin films prepared by dual reactive cosputtering” Advanced Materials, vol. 21, no. 5, pp. 593596, 2009.
[4] Y. Lu, M. Reusch, N. Kurz, A. Ding, T. Christoph, M. Prescher, L. Kirste, O. Ambacher, and A. Žukauskaitė, ”Elastic modulus and coefficient of thermal expansion of piezoelectric Al1-xScxN (up to x = 0.41) thin films,” APL Materials 6(7), 076105 (2018).
[5] Y. Ai, S. Yang, Z. Cheng, L. Zhang, L.Jia, B. Dong, J. Wang, and Y. Zhang, “Enhanced performance of AlN SAW devices with wave propagation along the ⟨1120⟩ direction on c-plane sapphire substrate”,J. Phys. D: Appl. Phys. 52 (2019)
[6] M. Loschonsky, D. Eisele, A. Dadgar, A. Krost, S. Ballandras, L. Reindl “Investigations of a-plane and c-plane GaN-based Synchronous Surface Acoustic Wave Resonators”, IEEE Int. Freq. Control Symp. 320325 (2008)
[7] J. Xu, Y. Wang, Z. Jia, Y. Xie, “Study on characteristics of Surface Acoustic Wave based on (110)ScAlN/R-sapphire structure”, Symposium on Piezoelectricity, Acoustic Waves, and Device Applications, Chengdu, Sichuan, China, pp. 519-523 (2017)
[8] N. Kurz, A. Ding, D. F. Urban, Y. Lu, L. Kirste, N. M. Feil, A. Žukauskaitė, O. Ambacher, “Experimental determination of the electro-acoustic properties of thin film AlScN using surface acoustic wave resonators” J. Appl. Phys. 126, 075106 (2019)
[9] D. F. Urban, C. Elsaesser, and O. Ambacher, “First-principles-calculation of electroacoustic properties of wurtzite (Al, Sc)N”(in preparation)
[10] A. Auld, Acoustic Fields and Waves in Solids, 2nd ed. Florida, Robert E. Krieger Publishing Company, 1990.
[11] A. F. Wright, “Elastic properties of zinc-blende and wurtzite AlN, GaN, and InN” J. Appl. Phys. 82, 2833 (1997)
[12] H.J. Bunge, Texture analysis in materials science: mathematical methods. Butterworth and Co, 1982.
[13] K. Dovidenko, S. Oktyabrsky, J. Narayan, “Aluminum nitride films on different orientations of sapphire and silicon” J. Appl. Phys. 79, 2439 (1996)
[14] L. B. Freund, S. Suresh, Stress, Defect Formation and Surface Evolution, 2nd ed. Cambridge, Cambridge University Press , 2010.
[15] U. C. Kaletta, C. Wenger, “FEM simulation of Rayleigh waves for CMOS compatible SAW devices based on AlN/SiO2/Si(100)” Elsevier Ultrasonics 54 (2014)